Formation of Silver-PAMAM Dendrimer Nanocomposites Using Electromagnetic Radiation

Igoris PROSYČEVAS[1*], Asta TAMULEVIČIENĖ[1], Asta GUOBIENĖ[1,3], Diana ADLIENĖ[2], Judita PUIŠO[1,2], Oleg ABDRAKHMANOV[4]

[1]*Institute of Physical Electronics of Kaunas University of Technology, Savanorių av. 271, Kaunas LT-50131, Lithuania*
[2]*Department of Physics, Kaunas University of Technology, Studentų str. 50, Kaunas LT-51368, Lithuania*
[3]*International Studies Centre, Kaunas University of Technology, Mickevičiaus str. 37, LT-44244, Kaunas, Lithuania*
[4]*Laboratory for Environmental Health Research, Institute for Biomedical Research, Kaunas University of Medicine,
 Eiveniu 4, LT-50161 Kaunas, Lithuania*

In the present research silver – polyamidoamine (PAMAM) dendrimer (with amino surface groups) nanocomposites were formed by UV irradiation. The formation of silver nanoparticles was monitored by UV-VIS spectroscopy. It is shown that the UV irradiation is a productive formation method. Formed nanocomposites were transferred onto the solid substrates (silica covered with polymer (polycarbonate or polymethylmethacrylate) layer). Solutions of nanocomposites and samples with transferred nanocomposites were exposed to irradiation by γ rays. The effect of radiation was analyzed considering the optical (UV-VIS spectra) and AFM measurements. It was shown that high energy photons induced changes of the size of nanocomposites in the solution and the morphology of the transferred nanocomposites.
Keywords: polyamidoamine (PAMAM) dendrimers, nanocomposites, UV irradiation, γ rays.

1. INTRODUCTION

Silver nanoparticles show remarkable optical properties that depend on their size and shape. They can be used as optical biomarkers because they exhibit significant advantages over alternative markers. Metal biomarkers are good candidates for cancer diagnostics. When gold or silver nanoparticles are conjugated to cancer antibodies, cancer cells are marked with those particles and every cell can be detected under a simple microscope due to their enhanced scattering properties [1]. In the dispersions metal nanoparticles must be stabilized to protect the aggregation. The stabilizers not only protect the nanoparticles from coagulation but also control the size of the metal particles in the course of synthesis [2]. Shape of nanoparticles can be controlled entrapping them into polymers. Polymers terminate the growth of the particles by controlling their nucleation [1].

Dendrimers, first synthesized by Tomalia in 1985 [3], represent a new structure of synthetic macromolecules. Unlike linear polymers, dendrimers are composed of a core molecule, hyperbranches, which regularly extend from the core, and terminal groups. Thus dendrimers have a definite molecular weight and size. In addition, dendrimers of higher generations ($G \geq 4$) take spherical shape and they can encapsulate metal complexes, nanoparticles, or other inorganic and organic guest molecules [2].

Since the 1990s dendrimers have also been studied as a stabilizer of metal nanoparticles. Dendrimers stabilize nanoparticles through adsorption on the coordinately unsaturated surface atoms or by incorporating the particles into their interior pores [4]. The application of different dendrimers has opened a new way of producing metal particles with small size and narrow particle distribution [5].

Dendrimer metal nanocomposites are novel hybride materials that display unique physical and chemical properties as a consequence of the atomic/molecular level dispersion of inorganic and organic molecules [6]. In their synthesis, dendrimers are used as templates to pre-organize metal ions followed by an in-situ reduction, which will immobilize and stabilize atomic domains of the reaction product(s). Size, shape, size distribution and surface functionality of these nanocomposites are determined and controlled by the dendritic macromolecules and may also be influenced by the encapsulated compounds. Solubility of these molecular nanocomposites is controlled by the polymer. Thus, it is possible to solubilize conventionally insoluble inorganic compounds in water or other solvents using dendritic hosts. The specific structure makes dendrimers suitable for a variety of biomedical applications. Among them, the use of dendrimers as carrier molecules for drugs has been of great interest [7].

The aim of this work is to study the possibilities of producing nanoparticles whose size is controlled by the functionality and size of the dendrimer. Also, the UV and gamma irradiation method permits continuous control of the concentration of the particles formed without the addition of reducing agents to the system.

2. EXPERIMENTAL

2.1. Materials and formation routes

The generation 5 PAMAM dendrimers with amino ($PAMAM(NH_2)_{128}$, 5 wt.% solution in methanol) surface groups and silver nitrate ($AgNO_3$) were obtained from Sigma Aldrich. All the chemicals and materials were of analytical grade. No further purification was performed.

---
[*]Corresponding author. Tel.: +370-37-313432; fax: +370-37-314423.
E-mail address: *igorpros@mail.ru* (I. Prosyčevas)

The silver nitrate solutions were prepared at 0.01 mM, 0.05 mM, 0.1 mM concentrations. Silver-PAMAM dendrimers composites were produced by irradiation with ultraviolet (UV) light. Mercury (Hg) lamp (30 W) was used as UV light source ($\lambda = 200$ nm $- 400$ nm). The distance between the quartz cell with mixed solution of dendrimer with silver nitrate (500 μl $AgNO_3$ and 20 μl $PAMAM(NH_2)_{128}$) and UV source was 0.10 m, irradiation duration – 80 min. Such duration was chosen according to other authors results [5].

The identification of Ag-PAMAM nanocomposites were performed according to dendrimer name and silver nitrate concentration. The used nomenclature is listed in Table 1.

Table 1. Identification of silver-PAMAM nanocomposites.

Concentration of $AgNO_3$, mM	Name of the silver-PAMAM composite
0.01	$\{(Ag^0)PAMAM\}0.01$
0.05	$\{(Ag^0)PAMAM\}0.05$
0.10	$\{(Ag^0)PAMAM\}0.1$

Solutions of the nanocomposites and silver-PAMAM composite layers were irradiated by γ rays. Co^{60} source ($E = 1.25$ MeV) was used as a gamma ray source. The dose rate of the source was 0.35 Gy/min. Distance between the source and sample – 75 cm, absorbed doze per sample – 2 Gy, exposition time – 342 s.

Ag-PAMAM composites were deposited on polymer modified silica substrate [8]. 20 μl of 2.5 % polycarbonate (PC) and 2.5 % polymethylmethacrylate (PMMA) were spincoated (2000 rpm, time – 12 s, drying in vacuum chamber ($p = 10^{-3}$ Pa) for 30 minutes) on the SiO_2 substrates. 100 μl of Ag-PAMAM nanocomposite solution was spread over the surface on modified silica substrate and irradiated with γ rays.

2.2. Analytical Techniques

The UV-VIS light spectrophotometer (Avantes 2048) was used for determination of silver nanocomposites formation, measuring optical absorbance spectra. This spectrophotometer is composed of deuterium and halogen light source (AvaLight DHc) and spectrometer (Avaspec-2048) with a detection system of 2048 pixel charge coupled device (CCD). It is possible to use the spectrometer in region from 192 nm to 1100 nm with the resolution of 1.4 nm. The statistical parameters of absorbance spectra were determined approximating experimental data assuming that they are distributed according to Gaussian law. The approximation was done employing "IgorPro 6.0" software [9].

Morphology of the structures deposited on silica substrates was investigated with an atomic force microscope (NANOTOP-206) operating in a contact mode (cantilever force constant 3 N/m).

3. RESULTS AND DISCUSSIONS

3.1. Formation of silver-PAMAM nanocomposites

The formation of Ag-PAMAM nanocomposites was monitored by UV-VIS light spectroscopy, measuring optical absorbance spectra. The absorbance peak (surface

plasmon resonance peak (SPR)) corresponding to silver nanoparticles wasn't observed in initial Ag-PAMAM components. This mentioned SPR peak was observed only after UV irradiation in optical absorbance spectra (see Fig. 1). The SPR peaks of 0.1 mM and 0.05 mM solutions were centred at 464.57 nm and 426.9 nm respectively. The absence of peak in the solution of 0.01 mM of silver nitrate concentration could be explained by weak silver nitrate concentration. The peaks centred at 250 nm $- 275$ nm are attributed to the silver ions Ag^+.
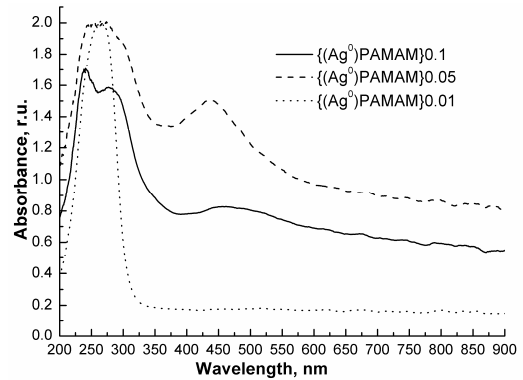

Fig. 1. UV-VIS spectra of solution of Ag-PAMAM nanocomposites after UV irradiation

The statistical parameters (SPR position, full width at half maximum (FWHM), absorbance intensity (AI)) of the curves were determined using "IgorPro 6.0" software. The results are summarised in Table 2.

Table 2. Statistical parameters of Ag-PAMAM nanocomposites

Sample	AI, r.u.	SPR, nm	FWHM, nm
$\{(Ag^0)PAMAM\}0.1$	0.18	464.57	117.36
$\{(Ag^0)PAMAM\}0.05$	0.58	426.90	118.02

One can see that the size of silver nanoparticles is dependent on the concentration of silver nitrate. Increase of silver nitrate concentration induced the SPR redshift, but stable FWHM values indicate the similar size distribution of nanoparticles in both cases.

3.2. Exposition of nanocomposite solutions to γ rays

It is well known that very narrow metallic (Ag) cluster size distributions in the solutions can be obtained by radiolysis [10]. Fig. 2 spectra illustrate the gamma rays irradiation effect on Ag-PAMAM nanocomposites.

Due to irradiation the intensity of SPR peak increased from 0.8 a.u. to 1.6 a.u. ($\{(Ag^0)PAMAM\}0.1$) that allows to conclude that the γ rays have induced further formation of silver nanoparticles. Analysing the results of the solution $\{(Ag^0)PAMAM\}0.05$ one can see the decrease of a background in the spectra, but the intensity (after the subtracting the background) and position of the peak remains stable.

The behaviour of peaks situated at 200 nm $- 275$ nm gives information about the formation steps of nanoparticles. In the case of $\{(Ag^0)PAMAM\}0.1$ solution

the irradiation with the high energy photons the absorption peak situated at ~300 nm diminishes and the one situated at 225 nm increases. For the solution of $\{(Ag^0)PAMAM\}0.05$ the peak centred at ~275 nm splits into two sharp peaks at 225 nm and 275 nm. These two peaks are located almost at the same positions as for the solution $\{(Ag^0)PAMAM\}0.1$ before irradiation. The peak at 225 nm can be attributed to the initial $AgNO_3$ [11] and the peak at 275 nm can be attributed to the appearance of clusters of silver ions Ag_2^+ in the nanocomposite solution [12]. One could conclude that the exposure of the solution to high energy photons induces the formation of silver nanoparticles and clustering of silver ions.
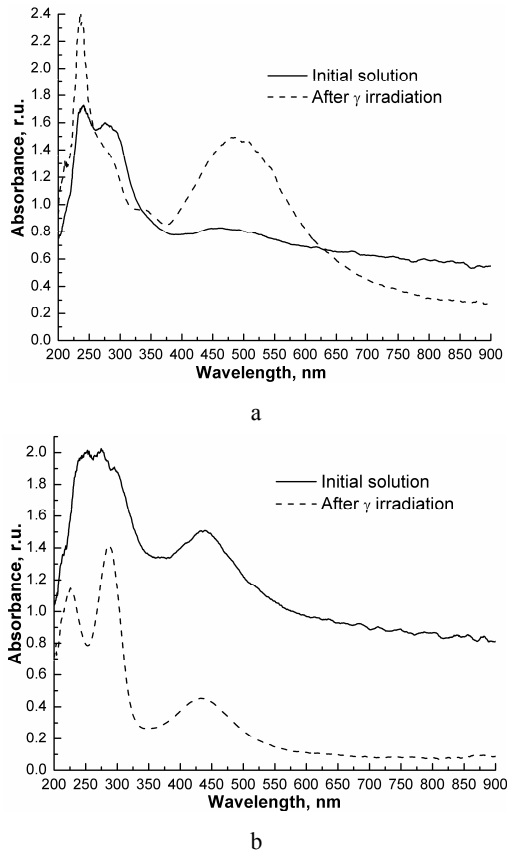

a

b

Fig. 2. UV-VIS spectra of Ag-PAMAM nanocomposites before and after γ irradiation ($E = 1.25$ MeV, 2 Gy): a $-$ $\{(Ag^0)PAMAM\}0.1$; b $-$ $\{(Ag^0)PAMAM\}0.05$

3.3. Silver-PAMAM nanocomposite transfer on solid substrates and exposition to γ rays

Optical spectra of Ag-PAMAM layers on silica substrate modified with polymers are presented in Fig. 3.

The SPR peaks in the spectra of nanocomposites solutions and its layers indicate presence of silver nanoparticles. Transferring of silver nanocomposites from solution to the solid phase induced the SPR peak shift. For the $SiO_2 + 2.5$ % $PC\{(Ag^0)PAMAM\}0.05$ (such notation means that Ag-PAMAM liquid was transferred on SiO_2 modified with 2.5 % PC), the peak is slightly red shifted (~3 nm) and for $SiO_2 + 2.5$ % $PMMA\{(Ag^0)PAMAM\}0.1$, the peak is blue shifted for approximately 30 nm. The shifts of the peaks are attributed to the local changes of refractive index of the surrounding material.
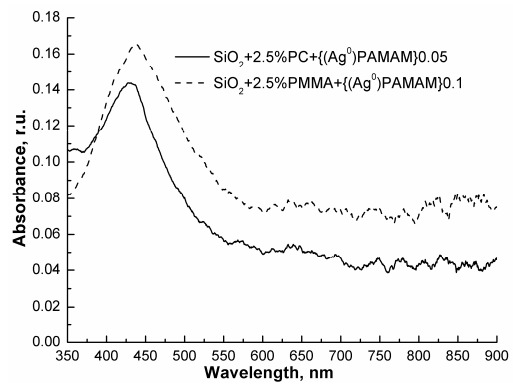

Fig. 3. UV-VIS spectra of Ag-PAMAM nanocomposites layers on silica substrates

The irradiation by γ rays also induced changes in the optical spectra of the samples. The intensity of the peak (Fig. 4, a) is lower and SPR peak became broader in comparison with the initial Ag-PAMAM layers. It allows predicting that γ rays have induced aggregation of small silver nanoparticles. The size distribution of silver nanoparticles became wider as the peak broadened. We could propose that the silver nanoparticles growth is originated from the smaller particles and those, which were originated from the UV irradiation are stable. Fig. 4, b, presents spectra of nanocomposite with the smaller silver concentration. It seems that the γ rays have induced further formation of silver particles. The intensity of the SPR peak became higher and the peak became more symmetric.
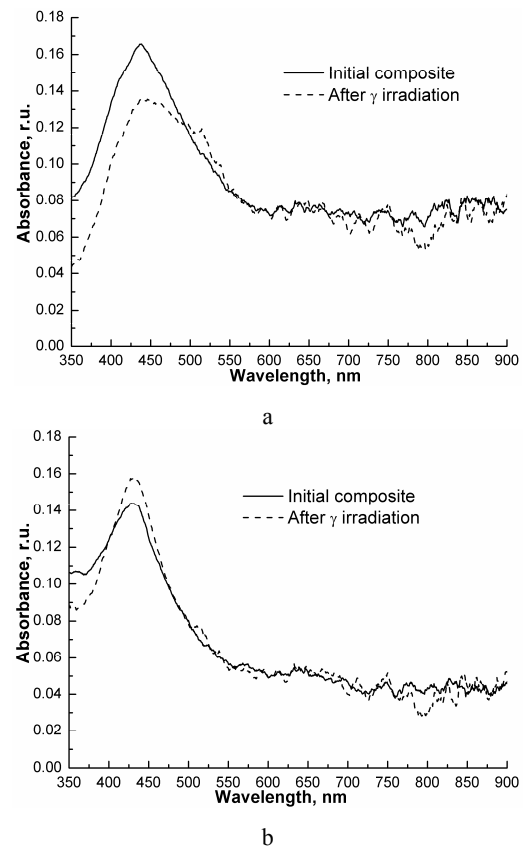

a

b

Fig. 4. UV-VIS spectra of Ag-PAMAM nanocomposites on solid substrates before and after γ irradiation ($E = 1.25$ MeV, 2 Gy): a $-$ $SiO_2 + 2.5$ % PMMA $\{(Ag^0)PAMAM\}0.1$, b $-$ $SiO_2 + 2.5$ % PC $\{(Ag^0)PAMAM\}0.05$

a   b   c
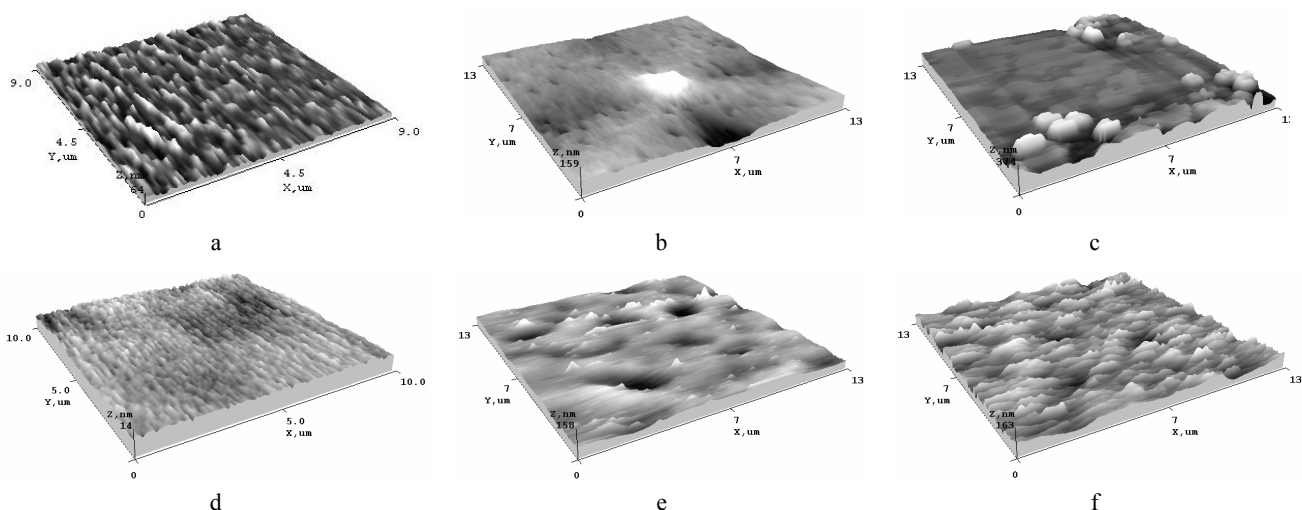
d   e   f

Fig. 5. AFM images of polymers and nanocomposites on SiO$_2$ substrates: a – 2.5 % PMMA; b – 2.5 % PMMA{(Ag^0)PAMAM}0.1 before γ irradiation; c – 2.5 % PMMA{(Ag^0)PAMAM}0.1 after γ irradiation; d – 2.5 % PC; e – 2.5%PC{(Ag^0)PAMAM}0.05 before γ irradiation; f – 2.5%PC{(Ag^0)PAMAM}0.05 after γ irradiation

Table 3. Statistical parameters of polymers and nanocomposite structures

Sample	R_a, nm	R_q, nm	Z, nm
2.5 % PMMA	5.8	7.6	64.1
2.5 % PC	0.7	0.9	14.1
SiO$_2$ + 2.5 % PMMA + {(Ag^0)PAMAM}0.1 before γ irradiation	7.9	12.9	158.9
SiO$_2$ + 2.5 % PC + {(Ag^0)PAMAM}0.05 before γ irradiation	8.0	11.5	158.3
SiO$_2$ + 2.5 % PMMA + {(Ag^0)PAMAM}0.1 after γ irradiation	20.5	31.5	373.8
SiO$_2$ + 2.5 % PC + {(Ag^0)PAMAM}0.05 after γ irradiation	9.1	12.3	122.8

Abbreviations: Z – maximum height, R_a – roughness average, R_q – root mean square roughness.

The morphology of Ag-PAMAM nanocomposites were investigated by AFM. The AFM pictures are shown in Fig. 5.

The investigation of roughness parameters were performed during all the formation process: polymer layers on SiO$_2$ substrate, deposition of Ag-PAMAM nanocomposite on polymer and irradiation with γ rays. All these parameters are summarized in Table 3.

One can see that the roughness drastically increases when on the Ag-PAMAM composite is deposited on SiO$_2$ + 2.5 % PC substrate. It increases more than 10 times. One can see from AFM images (Fig. 5, d and e)) that after the Ag-PAMAM deposition sharp structures which could be attributed to the nanocomposite particles are visible on the surface. The irradiation with high energy photons has little influence on the roughness parameters.

Analysing the results for other samples – modified with PMMA, one can see that the deposition of Ag-PAMAM nanocomposite does not change the roughness parameters so drastically as in case of PC. The higher increase is visible after the irradiation with γ rays. It is clear from the AFM image, that the irradiation induces aggregation of smaller silver nanoparticles, which was also predicted from the UV-VIS spectra.

CONCLUSIONS

We have shown that Ag-PAMAM nanocomposites can be successfully synthesized using UV irradiation. The irradiation of the Ag and PAMAM solutions with high energy photons (γ rays) produced silver nanoparticles in the PAMAM matrix.

Silver-PAMAM nanocomposites were successfully transferred from solution into solid phase on modified silica. Gamma radiation has induced changes in optical properties and surface morphology of Ag-PAMAM nanocomposites.

REFERENCES

1. **Courrol, L. C., Oliveira Silva, F. R., Gomes, L.** A Simple Method to Synthesize Silver Nanoparticles by Photo-reduction *Colloids and Surfaces A: Physicochemical Engineering Aspects* 305 2007: pp. 54 – 57.

2. **Torigoe, K., Suzuki, A., Esumi, K.,** Au(III)-PAMAM Interaction and Formation of Au-PAMAM Nanocomposites in Ethyl Acetate *Journal of Colloid and Interface Science* 241 2001: pp. 346 – 356.

3. **Tomalia, D. A., Baker, H., Dewald, J., Hall, M., Kallos, G., Martin, S., Roeck, J., Ryder, J., Smith, P.** A New Class of Plymers: Starburst-dendritic Macromolecules *Polymer Journal* 17 (1) 1985: pp. 117 – 132.

4. **Endo, T., Yoshimura, T., Esumi, K.** Synthesis and Catalytic Activity of Gold-silver Binary Nanoparticles Stabilized by PAMAM Dendrimer *Journal of Colloid and Interface Science* 286 2005: pp. 602 – 609.

5. **Kéki, S., Török, J., Deák, G., Daróczi, L., Zsuga, M.** Silver Nanoparticles by PAMAM-Assisted Photochemical Reduction of Ag^+ *Journal of Colloid and Interface Science* 229 2000: pp. 550 – 553.

6. **Atwater, J. E., Akse, J. R., Holtsnider, J. T.** Cobalt-poly(amido amine) Superparamagnetic Nanocomposites *Materials Letters* 62 2008: pp. 3131 – 3134.

7. **Klajnert, B., Sadowska, M., Bryszewska, M.** The Effect of Polyamidoamine Dendrimers on Human Erythrocyte Membrane Acetylcholinesterase Activity *Bioelectrochemistry* 65 2004: pp. 23 – 26.

8. **Šileikaitė, A., Prosyčevas, I., Puišo, J., Juraitis,A., Guobienė, A.** Analysis of Silver Nanoparticles Produced by Chemical Reduction of Silver Salt Solution *Materials Science* (*Medžiagotyra*) 12 (4) 2006: pp. 287 – 291.

9. http://www.wavemetrics.com/ (status of 2008-07-20).

10. **Gutierez, M., Henglein, A.** Formation of Colloidal Silver by "Push-Pull" Reduction of Ag^+ *The Journal of Physical Chemistry* 97 (44) 1993: pp. 11368 – 11370.

11. **Šileikaitė, A., Puišo, J., Prosyčevas, I., Tamulevičius, S.** Investigation of Silver Nanoparticles Formation Kinetics during Reduction of Silver Nitrate with Sodium Citrate *Materials Science* (*Medžiagotyra*) 15 (1) 2009 pp. 21 – 27.

12. **Ershov, B. G., Janata, E., Henglein, A., Fojtik, A.** Silver Atoms and Clusters in Aqueous Solution: Absorption Spectra and the Particle Growth in the Absence of Stabilizing Ag^+ ions *Journal of Physical Chemistry* 97 (18) 1993: pp. 4589 – 4594.